NCAR | EARTH OBSERVING LABORATORY

CFACT

NCAR/EOL ISFS Surface Meteorology and Flux Products Data Report

Dr. Steven Oncley
Prepared by Jacquelyn Witte

Earth Observing Laboratory
In situ Sensing Facility

NATIONAL CENTER FOR ATMOSPHERIC RESEARCH
P.O. Box 3000
BOULDER, COLORADO 80307-3000

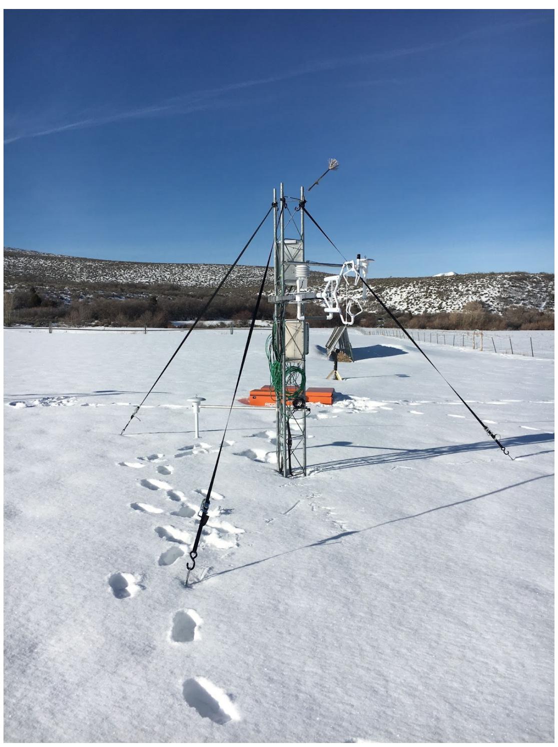

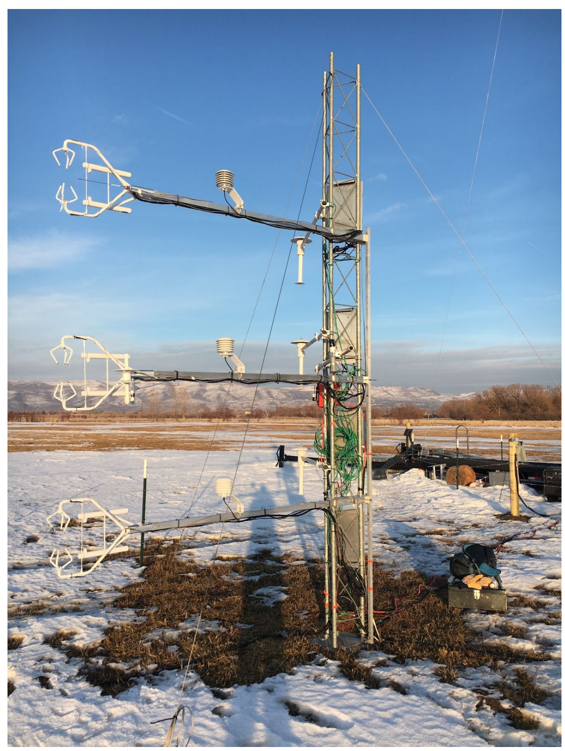

Table of Contents

CFACT Principal Investigators

Dr. Zhaoxia Pu - Zhaoxia.Pu@utah.edu
Dr. Eric Pardyjak - pardyjak@mech.utah.edu

Dept. of Atmospheric Sciences
University of Utah
Salt Lake City, UT 84112-0110
USA

EOL ISFS Staff

ISFS Lead Scientist: Steven Oncley <oncley@ucar.edu>
Engineers: Chris Roden, Gary Granger, Isabel Suhr
Technicians: Dan Buonome, Anthony Weise
Data Managers/Associate Scientists: Jacquelyn Witte <jwitte@ucar.edu>, Matthew Paulus

Web References

CFACT Homepage: https://www.eol.ucar.edu/field_projects/cfact
CFACT Field Catalog: https://catalog.eol.ucar.edu/cfact
ISFS Operations during CFACT: https://www.eol.ucar.edu/content/isfs-operations-cfact
ISFS Homepage: https://www.eol.ucar.edu/node/152
Calculation of long-wave radiation:
https://www.eol.ucar.edu/content/calculation-long-wave-radiation

Visualization Resources

- NCharts: Winds in geographic, Leica tilt corrected coordinates
- NCharts: Winds in geographic, planar tilt corrected coordinates
- CFACT ISFS Daily Data Statistics and Plots

Related Documentation

ISFS netCDF File Conventions: ISFS netCDF File Conventions
ISFS Guides: https://www.eol.ucar.edu/content/isfs-guides

Citations

If these data are used for research resulting in publications or presentations, please acknowledge EOL and NSF by including the following citations, as appropriate:

CFACT Data Sets

- NCAR/EOL ISFS Team. 2022. CFACT: NCAR/EOL ISFS **5-minute** Surface Meteorology and Flux Products - winds in **theodolite** geographic and tilt corrected coordinates. Version 1.0. UCAR/NCAR - Earth Observing Laboratory. https://doi.org/10.26023/X57X-SY8Y-N50J. Accessed 21 Nov 2022.

- NCAR/EOL ISFS Team. 2022. CFACT: NCAR/EOL ISFS **5-minute** Surface Meteorology and Flux Products - winds in **planar** geographic and tilt corrected coordinates. Version 1.0. UCAR/NCAR - Earth Observing Laboratory. https://doi.org/10.26023/PSTN-4RYP-570G. Accessed 21 Nov 2022.

- NCAR/EOL ISFS Team. 2022. CFACT: NCAR/EOL ISFS **High Rate** Surface Meteorology and Flux Products - winds in **theodolite** geographic and tilt corrected coordinates. Version 1.0. UCAR/NCAR - Earth Observing Laboratory. https://doi.org/10.26023/AAHW-XWQ1-F50J. Accessed 18 Nov 2022.

- NCAR/EOL ISFS Team. 2022. CFACT: NCAR/EOL ISFS **High Rate** Surface Meteorology and Flux Products - winds in **planar** geographic and tilt corrected coordinates. Version 1.0. UCAR/NCAR - Earth Observing Laboratory. https://doi.org/10.26023/V6YS-HG3P-HJ0G. Accessed 18 Nov 2022.

The ISFS Platform

- NCAR - Earth Observing Laboratory. (1990). NCAR Integrated Surface Flux System (ISFS). UCAR/NCAR - Earth Observing Laboratory. https://doi.org/10.5065/D6ZC80XJ.

Acknowledgement

Users of EOL data are expected to add the following acknowledgement to all of their publications, reports and conference papers that use those data:

“We would like to acknowledge operational, technical and scientific support provided by NCAR’s Earth Observing Laboratory, sponsored by the National Science Foundation.”

Overview

The Cold Fog Amongst Complex Terrain (CFACT) winter time fog study was conducted in Heber City Valley region, Utah and officially ran from 06 January - 23 February 2022. Data beyond the official period of the study are included to take advantage of fog events that occurred outside the official dates.

NCAR's Integrated Surface Flux System (ISFS) staff operated two 32m towered supersites with a full suite of flux and meteorological monitoring sensors, and nine 2 m satellite flux stations. An additional 3 m flux tower was added to both supersites instrumented with 3D sonic anemometers and h2o/co2 infrared gas analysers. Soil sensors to monitor heating and moisture parameters were operating at most sites. The PI's supplied additional sensors of snow depth, visibility, and thermocouple measurements that have been integrated into the ISFS data stream and included in the data sets.

ISFS flux and surface measurements during this project can contribute to 1) investigating cold fog development and environment conditions in complex terrain with the latest observation technology, 2) improving microphysical parameterizations and visibility algorithms used in numerical weather prediction (NWP) models.

Site Description

Eleven flux towers were operated throughout the Heber City valley region, Utah. Towers comprised two 3 m and 32 m multilevel flux profile Rohn towers and nine single low-level flux stations. Refer to the **Table 1** below for site locations and sensor configurations. **Figure 1** shows relief map rendition of the sites deployed around the Heber City valley region.

Figure 1. Google Map rendering of site locations is provided below.

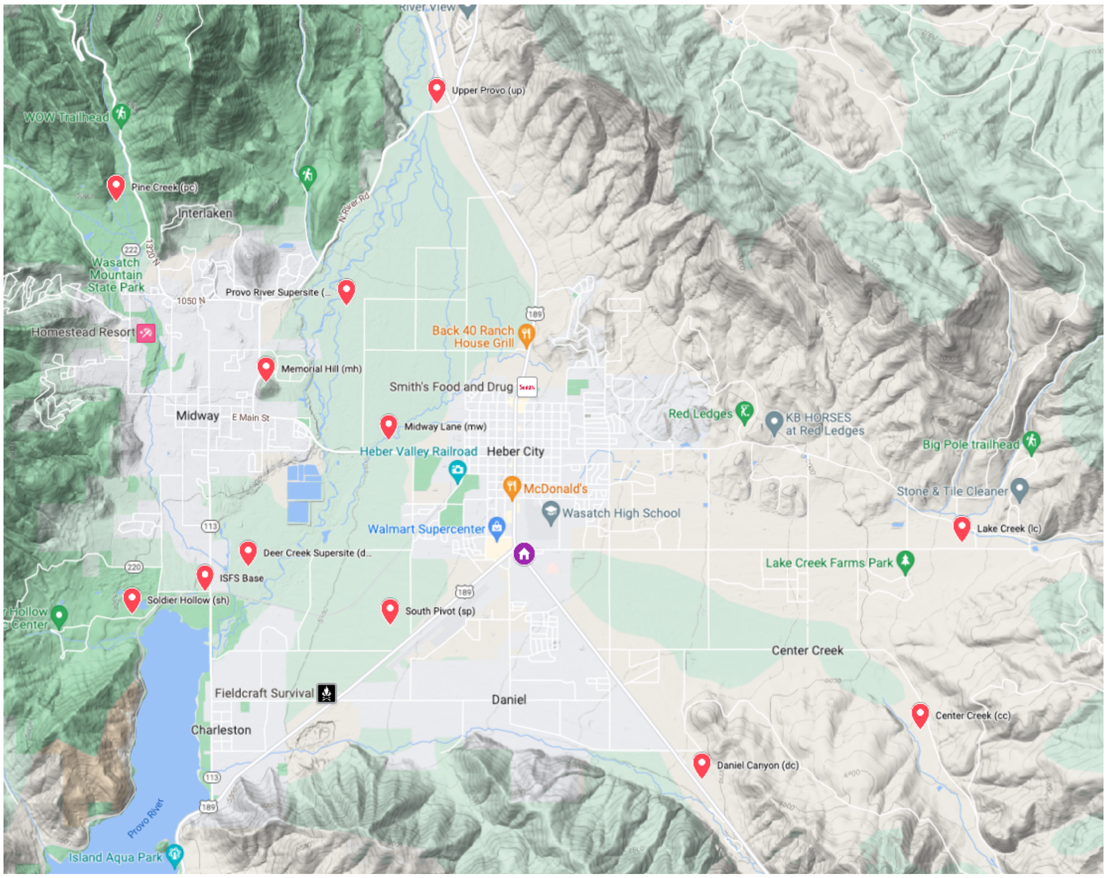

Table 1. Sites and locations. The abbreviated short name is used in the netCDF sitename definition.

Site	Short Name	Nominal Heights [m]**	Latitude	Longitude
Center Creek	cc	2	40.466344	-111.335625
Daniel Canyon	dc	2	40.459124	-111.37758
Deer Creek Supersite	dcs	0.5, 1, 2, 3, 7, 17, 32	40.490101	-111.464737
Lake Creek	lc	2	40.493671	-111.32765
Memorial Hill	mh	2	40.516918	-111.461368
Midway Lane	mw	2	40.508516	-111.437739
Pine Creek	pc	2	40.543386	-111.490119
Provo River Supersite	prs	0.5, 1, 2, 3, 7, 17, 32	40.528118	-111.445836
Soldier Hollow	sh	2	40.483202	-111.487092
South Pivot	sp	2	40.481611	-111.437426
Upper Provo	up	2	40.55752	-111.42852

**Heights at which various sensors were mounted. Sensor configuration at each height is detailed in the Instrument Set-Up section.

Data Set Description

Project Period: 06 January - 24 February 2022
Data set Period: 04 December 2021 - 02 March 2022

Because we are including a longer time series please note that not all sites and sensors were operating outside the official project dates. The set-up period runs from 04 December 2021 to 05 January 2022. After 24 February, flux towers were taken down so data availability gradually diminished after that date.

Time period: 06 December 2021 - 02 March 2022
Location: Heber City, Utah
Data layout: ISFS netCDF File Conventions
Data file frequency: Daily
Data version: v1.0
Data access: public

5-minute data sets

Data format: netCDF3
Time resolution: 5-minute

Data set name	NCAR/EOL ISFS 5-minute Surface Meteorology and Flux Products - winds in **theodolite** geographic and tilt corrected coordinates
File name format	isfs_cfact_5min_qc_geo_tiltcor_grav_YYYYmmDD.nc
DOI	https://doi.org/10.26023/X57X-SY8Y-N50J

Data set name	NCAR/EOL ISFS 5-minute Surface Meteorology and Flux Products - winds in **planar** geographic and tilt corrected coordinates
File name format	isfs_cfact_5min_qc_geo_tiltcor_planar_YYYYmmDD.nc
DOI	https://doi.org/10.26023/PSTN-4RYP-570G

High Rate data sets

Data format: netCDF3
Time resolution: Varies from 50 ms for 20 Hz sensors to 1 s for 1 Hz sensors. Refer to Table 4 for sampling rates.

Data set name	NCAR/EOL ISFS High Rate Surface Meteorology and Flux Products - winds in **theodolite** geographic and tilt corrected coordinates
File name format	isfs_cfact_hr_qc_geo_tiltcor_grav_YYYYmmDD.nc
DOI	https://doi.org/10.26023/AAHW-XWQ1-F50J

Data set name	NCAR/EOL ISFS High Rate Surface Meteorology and Flux Products - winds in **planar** geographic and tilt corrected coordinates
File name format	isfs_cfact_hr_qc_geo_tiltcor_planar_YYYYmmDD.nc
DOI	https://doi.org/10.26023/V6YS-HG3P-HJ0G

3D Sonic Anemometer Geographic Coordinates and Tilt Corrections

The flux towers masts/tripods were constructed to face roughly parallel to the local height contours and the anemometer boom to be mounted on this face, i.e. wind from the un-obstructed direction. This was done to minimize distortion of the flow by the mast for winds perpendicular to the ridge lines and also capture up and down valley flows. The local slope direction varied over the domain, resulting in boom mounted anemometer angles over a large range of degrees (Refer to **Table 3** for compass measured boom angles). Also, local surrounding obstacles (trees, shrubs, poles, gates) may interfere with the anemometer at certain tower locations. In these cases, the anemometer boom was set to point down-valley. Refer to the companion photographic documentation for visualizations of the tower set-up scheme for each site.

In order to report winds in geographic coordinates, the orientation of the instrument needs to be known to rotate the wind vectors into geographic coordinates. With a measured azimuth angle taken along the boom mounted sonics, the orientation is known since every anemometer head is rigidly attached to the boom and the sonic heads are attached in a captive manner.

The tilt of a sonic anemometer from true vertical can introduce errors in the measured sensible heat and momentum fluxes. The tilt error in a scalar flux is on the order of 5% per degree of tilt in the vertical plane aligned with the mean wind direction. Consequently, it is often necessary to rotate the coordinates of three-dimensional sonic wind data to correct for this tilt.

Boom angles and tilt coordinates were calculated two ways by the

1. Sonic anemometer orientation corrected by the handheld compass, and
2. Sonic anemometer orientation corrected by the Leica laser scanning theodolite.

1. Planar geographic and tilt corrected coordinates

A hand-held compass was used to measure the direction along the anemometer boom looking into the tower with respect to the magnetic north. Compass angles have been converted to true headings using a magnetic declination of 6 degrees east.

We estimate the sonic tilt angles with respect to the flow through the sensors from the archived wind data using the planar fit technique described in Wilczak, Oncley, and Stage, 2001, "Sonic Anemometer Tilt Correction Algorithms," Boundary Layer Meteor., 99, pp. 127-150. These data sets are labeled as ‘planar’.

A mean offset in the measured vertical velocity is applied. The mean offsets in the horizontal wind vectors cannot be obtained by the planar fit technique, but they do not have a significant impact in the tilt corrections (Wilczak, Oncley, and Stage, 2001).

A list of reference material below provides information on tilt corrections and wind coordinates using compass bearings.

- Sonic tilt corrections - Processing of sonic anemometer data.
- Wind direction quick reference - Explanation of the wind coordinate system.
- Wilczak, J.M., Oncley, S.P. & Stage, S.A. Sonic Anemometer Tilt Correction Algorithms. Boundary-Layer Meteorology 99, 127–150 (2001). https://doi.org/10.1023/A:1018966204465

2. Theodolite geographic and tilt corrected coordinates

As part of the total survey of CFACT anemometer instrumentation, the Leica Multistation (MS60 laser theodolite) made scans of the positions and orientation of the sonic anemometers with respect to gravity. The scans were georeferenced using a stand-alone GPS receiver. These data sets are labeled as 'grav'.

The Leica theodolite measures distances relative to itself using a very precise laser and knowledge of its azimuth and elevation angle. The distances are measured in x, y coordinates, using the Universal Transverse Mercator (UTM) geodetic projection, and converted to true headings using a declination of 6 degrees. **Table 2** shows the comparison of Leica and compass azimuth angle calculations. **Table 3** shows the sonic orientations determined using **(A)** the compass and **(B)** the Leica. Tilt-corrected data have been produced using these values, and all data in geographic coordinates have used these azimuth angles.

Table 2. Azimuth angle calculations for the satellite sites.

Satellite Sites	Compass Azimuth [deg]	Leica Azimuth [deg]
cc	170	160
dc	330	317
lc	90	87
mh	160	161
mw	0	359
pc	190	184
sh	80	79
sp	182	203
up	190	191

Table 3. Heights, and sonic orientations by site determined by (A) compass bearings, and (B) the theodolite. 'w offset' in (A) is the mean offset in the measured vertical velocity.

(A)

Site short name	Height [m]	Compass Bearing into the boom [deg]	Pitch [deg]	Roll [deg]	Lean [deg]	Lean Azimuth [deg]	w offset [cm/s]
cc	2	237	0.0	0.0	1.4	-36.6	0
dc	2	39	0.0	0.0	2.3	75.8	0
lc	2	169	0.0	-0.1	2.9	-38.7	-1
mh	2	241	1.5	-0.9	6.9	178.8	14
mw	2	85	-0.9	-0.5	1.9	-11.2	0
pc	2	264	0.0	0.0	4.6	70.8	0
sh	2	162	0.0	0.0	1.8	80.5	-1
sp	2	278	-0.1	0.0	2.1	5.8	0
up	2	275	0.0	0.0	2.8	12.8	-1
prs	1	98	-0.1	0.0	0.1	-128	-4
	2	98	-0.4	-2.2	2.2	-66.2	-1
	3	98	0.1	0.3	1.3	-14.8	3
	7	267	0.0	-0.1	0.7	-9.4	2
	17	264	-0.3	-0.5	3.2	27.6	0
	32	269	0.0	-0.4	2.7	7.4	5
dcs	1	104	0.1	-0.2	0.7	-24.4	-8
	2	104	-0.2	-0.6	1.4	14.3	1
	3	104	-0.5	-0.3	1.2	56.6	4
	7	282	-0.3	-0.4	1.5	50.6	5
	17	279	0.4	-0.9	2.5	-9.2	4
	32	281	-0.7	-1.6	4.1	37.7	5

(B)

Site short name	Hgt (m)	Pitch [deg]	Roll [deg]	Lean [deg]	Lean Azimuth [deg]
prs	1.145	-0.15	-2.11	2.1	-85.8
	2.048	-1.08	10.48	10.5	84.1
	3.192	-0.75	-0.61	1	-39.2
	6.801	-0.31	-1.29	1.3	-76.7
	17.143	-2.21	-0.10	2.2	-2.7
	32.765	-0.06	4.55	4.5	89.3
dcs	1.076	-1.15	-0.44	1.2	-20.9
	2.004	-1.03	1.48	1.8	55
	3.137	-1.07	0.19	1.1	9.9
	6.762	-0.52	-0.35	0.6	-34.4
	16.874	-0.95	-0.69	1.2	-36.1
	31.971	-3.84	1.08	4	15.7

Data File Contents

Data files are provided in netCDF3 format. Research parameters contained in the 5-minute and high rate data are provided below.

Meteorological Variables

Variable name	Quantity Measured	unit	Instrument
P	Barometric Pressure	mb	Paroscientific 6000
T	Air Temperature	degC	Sensirion SHT85
RH	Relative humidity	%	Sensirion SHT85

3D Sonic Anemometer Variables

Instrument - Campbell Scientific CSAT3

Variable name	Quantity Measured	unit
u	Wind U component	m/s
v	Wind V component	m/s
w	Wind W component	m/s
spd	Wind speed	m/s
dir	Wind Direction	deg
tc	Virtual air temperature from speed of sound	degC
ldiag	logical diagnostic applied, 0=OK, 1=one or more non-zero diag bits	none

CO_2 and H_2O Open-Path Gas Analyzer Variables

Instrument - Campbell Scientific combination of EC100 and EC150 models

Variable name	Quantity Measured	unit
h2o	Water vapor density	g/m^3
co2	CO2 density	g/m^3
Pirga	Barometric pressure	mb
Tirga	Air temperature	degC
irgadiag	Sensor diagnostics applied, 0=OK, 1=one or more non-zero diag bits	none

Radiation Variables

All the satellite sites used the Hukesflux NR01 radiometers. The supersites used a combination of Hukseflux NR01 and Kipp&Zonen. At Deer Creek (dcs) and Provo River (prs) all of the height-specified variables are Kipp&Zonens, and those without height designation are Hukseflux NR01 instruments mounted at 2 m - just like the satellite sites.

Radiation data are not included in the high rate data due to the coarse time resolution. Refer to **Table 4** for sampling rates.

Variable name	Quantity Measured	unit	Instrument
Rsw_in	Incoming Shortwave	W/m^2	Kipp&Zonen, Hukesflux NR01
Rsw_out	Outgoing Shortwave	W/m^2	Kipp&Zonen, Hukesflux NR01
Rpile_in	Incoming Thermopile	W/m^2	Kipp&Zonen, Hukesflux NR01
Rpile_out	Outgoing Thermopile	W/m^2	Kipp&Zonen, Hukesflux NR01
Rlw_in	Incoming longwave	W/m^2	Kipp&Zonen, Hukesflux NR01
Rlw_out	Outgoing longwave	W/m^2	Kipp&Zonen, Hukesflux NR01
Rsum	Net radiation computed as the signed sum of the 4 components	W/m^2	Kipp&Zonen, Hukesflux NR01
Tcase	Case temperature	degC	Hukesflux NR01

Tcase_in	Case temperature	degC	Kipp&Zonen
Tcase_out	Case temperature	degC	Kipp&Zonen
Tsfc	Surface temperature, computed from Rlw_out	degC	Kipp&Zonen, Hukesflux NR01
Wetness	Leaf Wetness	V	Decagon

Note that Tsfc was computed using our standard code using an emissivity of 0.98, which may be a bit low for the predominantly snow-covered surfaces.

Soil Variables

Soil data are not included in the high rate data due to the coarse time resolution. Refer to **Table 4** for sampling rates.

Variable name	Quantity Measured	unit	Instrument
Gsoil	Heat flux	W/m^2	REBS HFT
Gsfc	Heat flux, extrapolated to the surface	W/m^2	HFT, TP01, Tsoil
Qsoil	Moisture	m^3/m^3	Meter EC-5
Tsoil	Temperature	degC	NCAR 4-level Tsoil
Lambda	Thermal conductivity	W/m/DegK	Hukseflux TP01
Tau63	Decay time constant	s	Hukseflux TP01
Csoil	Heat capacity computed from Lambda and asoil	$J/(m^3\ degC)$	Hukseflux TP01

Precipitation Variables

Precipitation data are not included in the high rate data due to the coarse time resolution. Refer to **Table 4** for sampling rates.

Instrument - OTT Parsivel2 Disdrometer

Variable name	Quantity Measured	unit
Rainr_ott	Rain rate	mm/h
WX_ott	Weather code according to SYNOP code*	-
Vis_ott	MOR visibility in precipitation	m
N_ott	Particle count	-

*For interpretation, refer to Appendix D of the Parsivel2 Operation Manual

PI-supplied Variables

Only the thermocouple data are included in the high rate data due. Refer to **Table 4** for sampling rates.

Variable name	Quantity Measured	unit	Instrument
T_cs	Temperature	degC	Campbell Scientific CS125
Vis_cs	Visibility	m	
Part_cs	Particle counts	count/min	
Rainr_cs	Precipitation intensity	mm/h	
SYNOP_cs	SYNOP code	-	
Depth_min	Snow depth	m	HRXL
t	Thermocouple Temperature	degC	Campbell Scientific FW1
tref	Thermocouple Reference Temperature	degC	

*Contact PI for the manufacturer

Dimension Variables

Variable name	Quantity Measured	unit
base_time	seconds since 1970-01-01 00:00:00 00:00	s
time	seconds since base_time	s

Higher Moments

We provide a long list of 2nd and 3rd moments among the winds, h2o, and co2. They follow the naming convention:

2nd moment: varname_varname__

3rd moment: varname_varname_varname__

For example,

```
float u_tc__sp(time) ;
        u_tc__sp:_FillValue = 1.e+37f ;
        u_tc__sp:long_name = "2nd moment" ;
        u_tc__sp:short_name = "u\'tc\'.sp" ;
        u_tc__sp:units = "m/s degC" ;
        u_tc__sp:counts = "counts_sp" ;

float w_w_tc__sp(time) ;
        w_w_tc__sp:_FillValue = 1.e+37f ;
        w_w_tc__sp:long_name = "3rd moment" ;
        w_w_tc__sp:short_name = "w\'w\'tc\'.sp" ;
        w_w_tc__sp:units = "(m/s)^2 degC" ;
        w_w_tc__sp:counts = "counts_sp" ;
```

Refer to the ISFS netCDF document which provides further detail on the ISFS instruments and their parameters, the netCDF naming convention, time sampling, and attributes.

Data Collection and Processing

All sensors were sampled independently with a Linux-based Data System Module or DSM. Data were stored directly onto USB sticks provided for every DSM. All DSMs were connected to a wireless network of Ubiquiti radios, so raw data could also be archived in real-time on a Linux laptop at the ISFS base trailer. Data were also transmitted from the base trailer to servers at EOL for local storage and added back-up. Data processing was performed by the in-house created data acquisition system called NIDAS.

NIDAS (NCAR In-situ Data Acquisition System) handles the data processing for all ISFS measurement systems. This is a linux based software produced by Gordon Maclean, formerly at NCAR/EOL. Each sensor is sampled independently. A time tag is assigned to each sample at the moment it is received, based on a system clock. Minimal data interpretation is performed to differentiate individual messages from a sensor, assembling the data exactly as it was received into a sample, with the associated time-tag and an identifier of the sensor and data system. The concatenated stream of samples from all sensors is then passed on for archival and further processing.

NIDAS reads a series of configuration and calibration files that contain pertinent sensor metadata and, more importantly, any input variables that are to be applied to the data either during operations or in the post-processing. NIDAS will also apply quality control flags and filters, and thresholds. To generate the 5-minute average and high rate data sets, NIDAS reads the variables from the raw information, applies calibrations and quality control filters, generates 5-minutes averages for those data sets, then writes the variables to a netcdf.

- Further introduction to NIDAS and access to the software can be found on its GitHub Wiki.
- NIDAS version used in these data sets is v1.2-1667.

Instrument Description

Most sites were instrumented for basic meteorology, eddy covariance fluxes, radiation, and soil heating and moisture. The standard 5-min and high rate ISFS products include measurements from the following sensors listed in **Table 4**. Included are PI-supplied sensors that have been added to the data sets.

All wetness sensors were coupled to each radiometer to filter incidences of moisture on the sensor dome, i.e. dew, rain, or snow.

Table 4. (A) ISFS sensors and description. **(B)** PI-supplied sensors and description. A subset of these sensor products (those sensors in **bold**) are in the high rate datasets.

Instrument	Manufacturer	Samples/s
Integrated Net Radiometer	4-component Hukseflux NR01	0.2
Pyranometer/Pyrgeometer	Kipp & Zonen	0.2
Wetness*	Decagon	0.2
Soil temperature profile sensor	NCAR 4-level Tsoil	0.2
Soil thermal properties - Decay time constant	Hukseflux TP01	0.2
Soil thermal properties - thermal conductivity	Hukseflux TP01	0.2
Soil Moisture	Meter EC-5	0.2
Heat flux plate	REBS HFT	0.2
Disdrometer	OTT Parsivel2	0.02
3D sonic anemometer	**Campbell Scientific CSAT3****	**20**
Hygrothermometer	**Sensirion SHT85**	**1**
H2O/CO2 Open-path InfraRed Gas Analyser (IRGA)	**Campbell Scientific (combination of EC100 and EC150)**	**20**
Nanobarometer	**Paroscientific 6000 Digiquartz**	**20**

**With the optional CSAT3A sonic anemometer head to couple with the IRGA EC150.

(B)

Sensor	Manufacturer	Samples/ second
Snow depth	HRXL-MaxSonar-WRS	0.15
Visibility (T, Rain rate parameters)	Campbell Scientific CS125	0.02
Thermocouple	**Campbell Scientific FW1**	**20**

Instrumentation set-up

Supersites

Deer Creek (dcs) and Provo River (prs) supersites were similarly instrumented. **Table 5** lists the sensors mounted at each height. **Photo 1** shows the instrument set-up for Deer Creek for illustration purposes. Heights were determined by the Leica survey instrument.

Table 5. Sensor configuration for each tower at the Deer Creek (DCS) and Provo River (PRS) Supersites.

Nominal Height (m)	Tower type	Sensors
-	-	All soil sensors
0.5m	Steel pole	Kipp&Zonen
1m	3m Rohn	3D sonic, h2o/co2, Thermocouple, Hygrothermometer, Visibility, Disdrometer
2m	3m Rohn	3D sonic, h2o/co2, Thermocouple, Hygrothermometer, nanobarometer
2m	Dark horse tripod	Hukseflux NR01, Kipp&Zonen
3m	3m Rohn	3D sonic, h2o/co2, Thermocouple, Hygrothermometer
7m	32m Rohn	3D sonic, h2o/co2, Thermocouple, Hygrothermometer, Kipp&Zonen
17m	32m Rohn	3D sonic, h2o/co2, Thermocouple, Hygrothermometer
32m	32m Rohn	3D sonic, h2o/co2, Thermocouple, Hygrothermometer, Kipp&Zonen

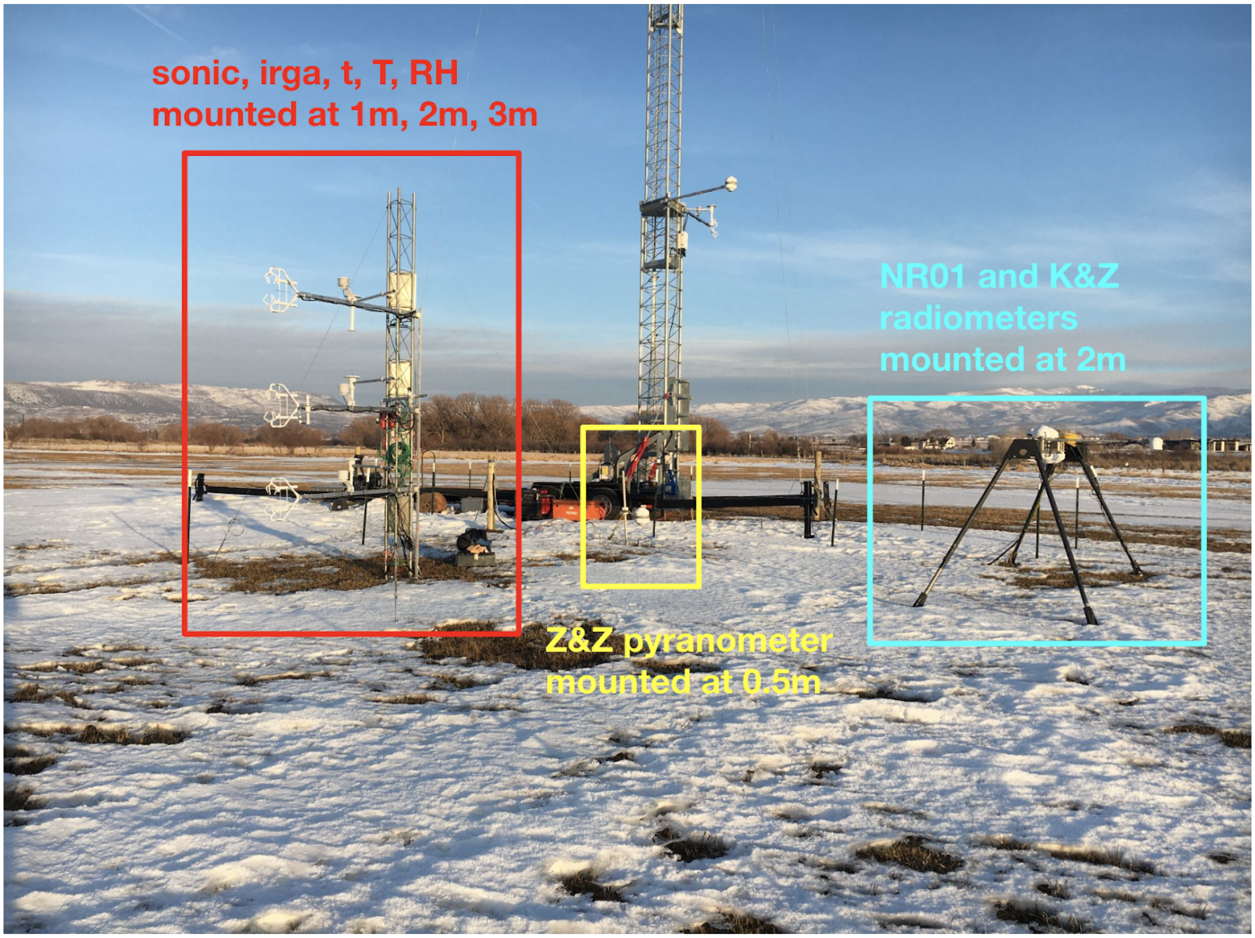

Photo 1. Deer Creek supersite instrument set-up. The 32 m flux tower is in the background. The configuration is similar to the Provo River supersite.

Satellite Sites

The satellite sites were similarly instrumented and contained the following sensors, with exceptions noted, in **Table 6**.

All satellite sites reached a nominal height of 2m. The radiometers and soils were set-up separately on tripods. Refer to **Photo 2** for a visual reference.

Refer to the CFACT site photos document that is included in the dataset landing page for visuals of the instrument orientation and surroundings.

Table 6. Sensor configuration at the satellite sites. All ambient sensors were mounted at 2m, except where noted. Radiometers were mounted separately on tripods.

Sensor	Special Notes
3D sonic anemometer	
H_2O/CO_2 InfraRed Gas Analyser	
Hygrothermometer	At heights 0.5m and 2m.
Nanobarometer	
Hukseflux NR01	None at mh.
All soil sensors	None at mh.
Disdrometer	
CS125 Visibility*	None at cc, dc, lc, pc, and up sites.
HRXL snow depth analyzer*	

*PI-supplied sensors

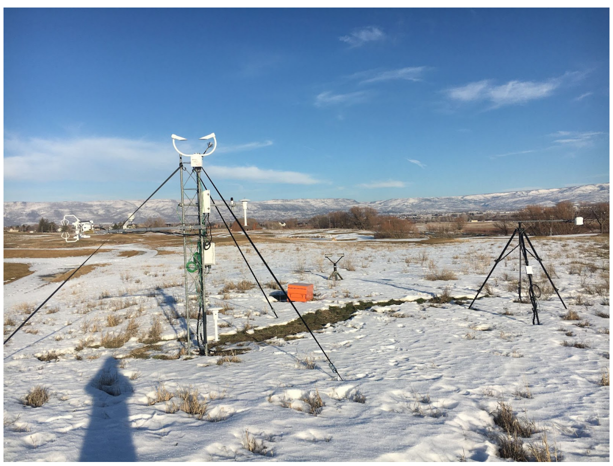

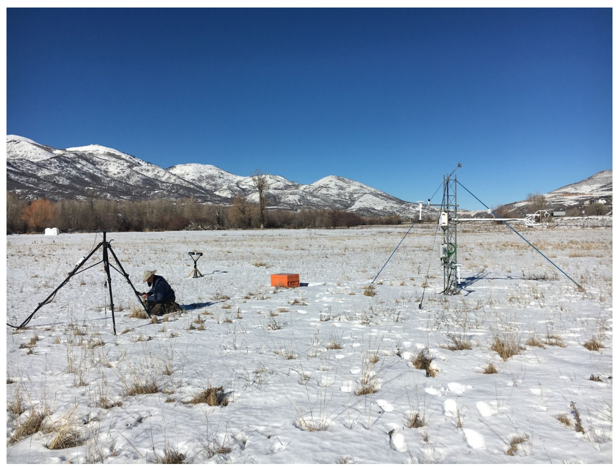

(A) **(B)**

Photo 2. Photos of Soldier Hollow (A) and Upper Provo (B) satellite sites showing a typical instrument set-up.

Data Availability

Figure 6 shows the percent of 5-minute ISFS sensor data remaining per variable after all quality checks and filters have been applied. The Memorial Hill site did not include a radiometer or soil sensors. Low percentages for Qsoil was due to filtering for frozen conditions (Refer to Soil Moisture data remarks below). Data availability of individual variables per site are provided in **Table 7**.

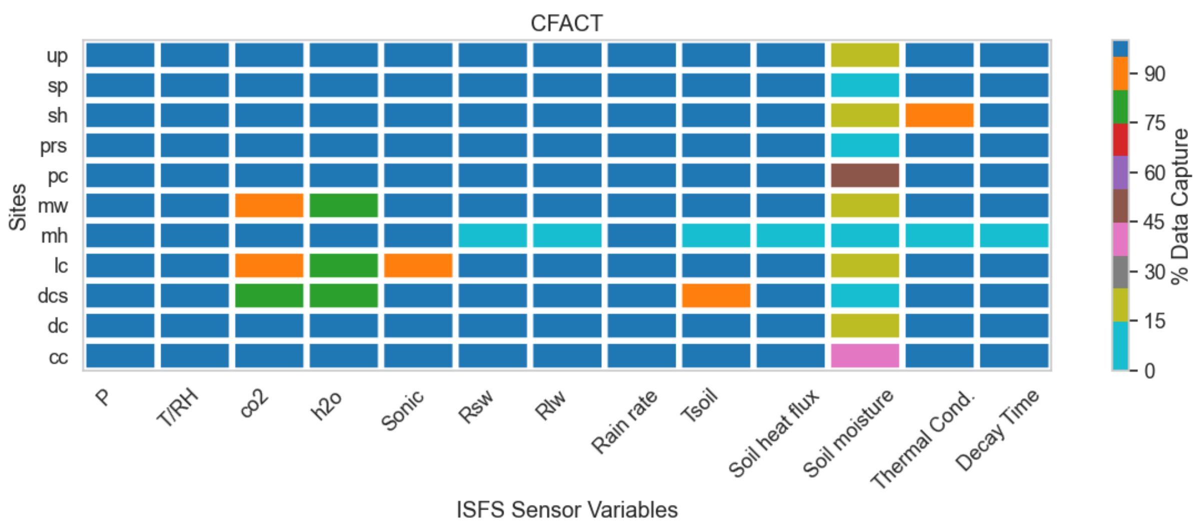

Figure 6. Percent of data available during the official start/stop (6 January - 23 February 2022) of CFACT. Most major ISFS sensor data sets are included.

Table 7. Data availability for the 5-minute data per site between 6 January - 23 February 2022. Empty cells indicate no instruments were operating at that site.

(A) Satellite sites

Site	P	T/RH	Radiometer	co2	h2o	sonic
cc	100	100	99.2	98.0	97.4	99.2
dc	96.9	96.9	96.7	93.6	92.9	96.7
lc	100	100	100	80.8	79.4	82.7
mh	100	100		95.0	93.6	97.1
mw	98.7	98.7	98.7	84.4	76.9	97.1
pc	100	100	100	93.3	93.2	98.5
sh	99.5	99.5	99.5	92.7	92.6	94.1
sp	99.8	99.8	99.8	96.2	94.2	98.3
up	99.2	99.2	99.2	93.6	93.4	98.6

(B) Supersites

Site	P	T/RH	Radiometer	co2	h2o	sonic	thermocouple
dcs_0.5m			100*				
dcs_1m		93.6		88.3	86.8	91.6	65.3
dcs_2m	99.5	99.5	100*	87.7	74.3	98.5	69.9
dcs_3m		99.5		93.9	91.0	98.3	92.6
dcs_7m		99.1	100*	75.9	70.7	97.6	81.4
dcs_17m		99.1		93.9	91.9	96.7	89.0
dcs_32m		99.1	100*	93.0	92.2	97.5	90.1
prs_0.5m			99.4				
prs_1m		99.4		81.3	76.2	98.3	70.0
prs_2m	99.8	99.5	99.4	86.6	85.0	93.9	53.1
prs_3m		99.8		89.1	84.9	98.2	91.0
prs_7m		98.9	96.3	94.5	91.7	97.5	86.6

prs_17m		99.1		96.3	95.5	97.9	88.0
prs_32m		99.1	98.8	95.5	93.7	97.5	79.2

*Radiometers were PI-supplied.

(C) Soils and precipitation

Site	Gsoil	Qsoil*	Tsoil	Lambda	Tau63	Rain rate	Visibility
cc	100	35.3	100	100	100	100	
dc	96.9	14.1	96.9	93.6	96.9	96.9	96.9
lc	100	14.9	100	100	99.0	100	
mh							100
mw	98.7	10.8	98.7	98.7	98.5	98.7	98.7
pc	100	47.5	99.6	100	100	100	
sh	99.5	10.3	99.5	87.9	99.3	99.5	99.5
sp	99.7	6.7	99.8	99.8	99.8	99.8	99.8
up	99.2	14.1	99.2	99.2	99.2	99.2	
dcs	92.8	0.0**	88.6	91.2	90.4	99.5	
prs	99.4	8.3	99.4	99.4	96.0	98.7	

*Low percentages for Qsoil was due to filtering for frozen conditions where Tsoil at 1.3 cm < 0.
**Bad measurements since installation.

Data Gaps

Small data gaps occur from time to time in a given sensors' data stream. These may be due to

- Loss of GPS signal when rebooting due to loss of power due to maintenance, i.e. servicing sensors.
- Sensor thresholds on the data.
- Status or error messages from the sensor

Data Quality Control

ISFS performed data quality checks on all ISFS sensors for consistency and anomalies. ISFS provided minimal data checks for PI-supplied instruments. Below we provide summaries of the QC workflow for each sensor.

While the CFACT project officially runs from 06 January - 23 February 2022, we have decided to include all data available from 04 December 2021 through 03 March 2022 to increase the number of fog-driven events that are of interest to the science team. Data came on-line gradually during the December set-up period and decreased after 23 February as sites were taken down.

The focus of this data report is the data quality control (QC) during the official period of the project. We provide data availability statistics for the 06 January - 23 February 2022 period only.

Supersite tower lowering/raising

Data measured from the 32 m flux towers were removed for the lowering/raising of these towers to replace broken thermocouples. Refer to **Table 5** for the list of instruments mounted on these towers.

Table 8. Dates and time when the 32 m towers were lowered and raised. Start and end times are taken from the 5-minute data set in UTC.

Site	Start time	End Time	Reason
dcs	Jan 07 21:57:30	Jan 07 23:32:30	Installed thermocouples
dcs	Jan 10 21:47:30	Jan 10 23:22:30	Replaced 7m thermocouple
dcs	Jan 26 20:47:30	Jan 26 22:22:30	Replaced 7m and 32m thermocouples
dcs	Jan 27 20:52:30	Jan 27 22:47:30	Replaced 32m thermocouple
dcs	Feb 11 19:02:30	Feb 11 20:07:30	Replaced 17m thermocouple
dcs	Feb 17 16:57:30	Feb 17 18:12:30	Replaced 7m thermocouple
dcs	Feb 23 18:12:30	Feb 23 18:12:30	Replaced thermocouples at all levels
prs	Jan 11 16:12:30	Jan 11 17:07:30	Replaced 7m thermocouple
prs	Jan 26 17:57:30	Jan 26 19:57:30	Replaced 32m thermocouple
prs	Feb 07 20:27:30	Feb 07 21:27:30	Replaced 17m thermocouple
prs	Feb 11 21:07:30	Feb 11 22:07:30	Replaced 7m thermocouple
prs	Feb 17 18:32:30	Feb 17 19:32:30	Replaced 32m thermocouple

Barometers

The Paroscientific nanobarometers were connected to All-Weather quad-disk probes and all pressure sensors worked as expected. No problems noted during operations. No problems were found during QC processing. No sensors were replaced during operations. Time series of all nanobarometers operating are plotted in **Figure 7**.

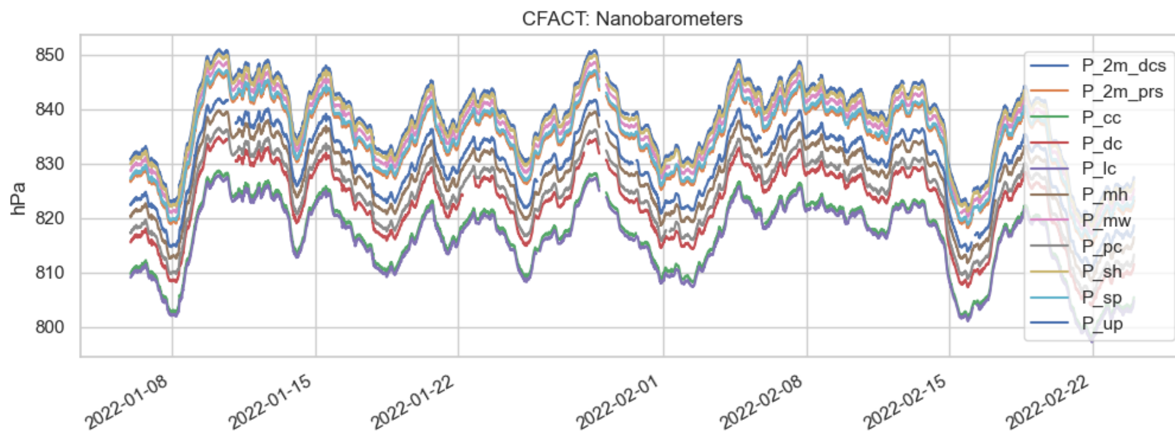

Figure 7. Time series of nanobarometers by site.

Hygrothermometer (T, RH)

Each tower used ventilated temperature/relative humidity sensors for vertical profiles. The fan speeds in the sensor housings were collected and used as an indicator that the sensor was functioning as expected. In general, the measurements were fairly stable. All the TRH sensors performed well. No problems noted during operations. No problems were found during QC processing. No sensors were replaced during operations. Time series of all TRH sensors by site are plotted in **Figure 8**.

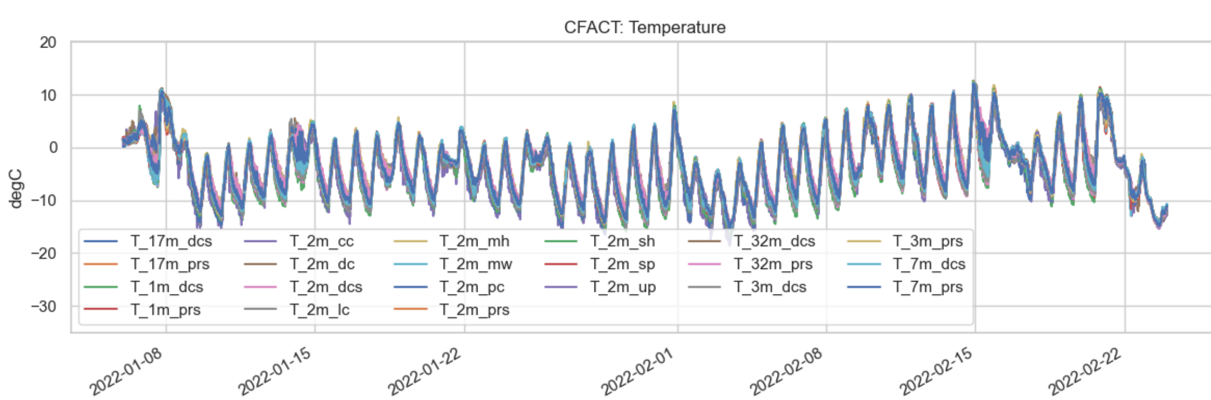

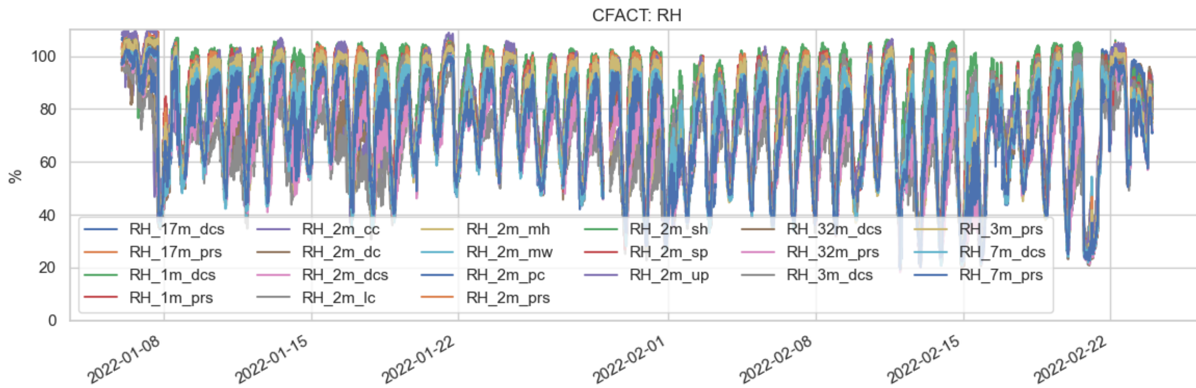

Figure 8. Time series of TRH sensors by site.

TRH Calibrations

Calibrations were done on the TRH sensors in the EOL Calibration Laboratory https://www.eol.ucar.edu/node/2652. Temperature oil baths were used to calibrate the temperature sensors and a Humidity Generator to calibrate the relative humidity sensors. Three constant temperatures were used to calibrate the RH; 1°C, 20°C, and 40°C. To evaluate the hysteresis effect the chamber RH was allowed to slowly increase from zero to near-100% then decrease back down to the zero. This process takes three days to complete. Eight RH probes were calibrated at a time. An example of a calibration plot is shown in **Figure 9**.

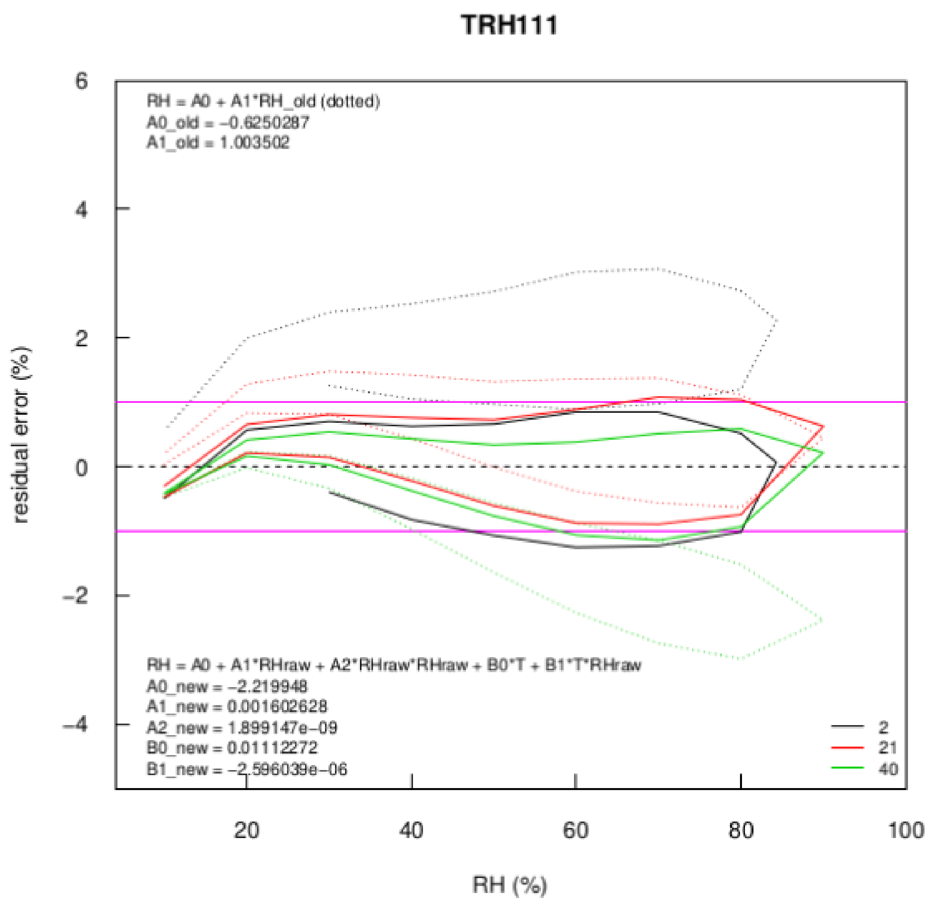

Figure 9. Post-calibration of RH for TRH sensor 111 at constant temperatures (1°C-black, 20°C-red, and 30°C-green). The curved shape is the result of measuring the increase then decrease of the known RH source at each temperature. The difference between the upper and lower bounds of the curve defines the hysteresis effect. Dotted lines are the percent residual error relative to a known source of RH before calibration. The solid lines are the adjustments to the fit to reduce the error to within 2%. Post campaign calibrations are the average of the three unadjusted curves and are included in the plot as A0_old (offset) and A1_old (gain). The final calibrated fits are the solid lines and fits to the average of post-calibrations are provided on the bottom left.

Pre-calibrations were completed in October and November 2021. All humidity sensors were calibrated to within ± 2% accuracy and all temperature probes were calibrated to within the expected error of ± 0.1°C.

Post-calibrations were completed by August 2022. ISFS conducted another field campaign on the heels of CFACT so it was not possible to conduct calibrations soon after CFACT. Post-calibrated temperature probes were within the expected error of +/- 0.1°C. A number of RH probes recorded errors greater than 2% relative to the reference. Most errors exhibited high bias between 20% and 80%, particularly at T=1°C. An overall hysteresis effect of 1% at constant T=1°C was observed. Fits to the RH reference are provided in **Table 9**.

Because post-calibrations were conducted well after CFACT and after another field campaign we do not know when the sensor accuracy diminished. However, comparisons of specific humidity from the sonic h2o and RH follow each other quite well (not shown). It was decided not to apply post RH calibration corrections to CFACT in **Table 9**.

Table 9. Post-calibration slope and offset fits to the RH reference based on equation RH = A0 + A1*RH_raw. A few RH sensors were not calibrated, however, none of these post RH calibrations have been applied.

Site	Hts	Serial No	RH fits
dcs	1	111	A0 = -0.6250287 A1 = 1.003502
dcs	2	107	-
dcs	3	5	A0 = -1.218166 A1 = 0.9646317
dcs	7	44	A0 = -0.4297421 A1 = 0.9194172
dcs	17	114	A0 = -0.612771 A1 = 0.9656231
dcs	32	106	A0 = -1.227657 A1 = 0.9766726
prs	1	128	A0 = -0.2605225 A1 = 0.9074223
prs	2	52	A0 = -0.8549647 A1 = 0.9775877
prs	3	122	A0 = -0.8358976 A1 = 0.9754848
prs	7	43	A0 = -1.126057 A1 = 1.003127
prs	17	112	A0 = -1.054596 A1 = 0.9482393
prs	32	21	A0 = -1.016343 A1 = 0.9704883
cc	2	1	A0 = -1.0229861 A1 = 0.9782945

dc	2	25	A0 = -0.6357728 A1 = 0.9136668
lc	2	3	A0 = -1.172988 A1 = 0.9645974
mh	2	45	A0 = -0.4237104 A1 = 1.229809
mw	2	29	A0 = -0.5502574 A1 = 1.007953
pc	2	118	A0 = -0.8049035 A1 = 0.9672272
sh	2	60	A0 = -0.9576032 A1 = 0.9855848
sp	2	109	-
up	2	58	-

Radiometers

Deer Creek and Provo River supersites used the Kipp & Zonen pyranometer/pyrgeometer sensor suite at heights 0.5 m, 2 m, 7 m, and 32 m. An NR01 Hukseflux 4-component radiometer was added at 2m at both supersites. All satellite sites used the NR01 radiometers mounted on darkhorse tripods at nominal heights of 2m. A wetness sensor was attached close to the sensors to record moisture levels.

Data have been filtered for

- Spikes
- Lowering/raising of the supersite towers for thermocouple replacement
- Moisture on the lens due to dew or precipitation as measured by the wetness sensors mounted on the NR01 radiometers at 2 m.

All longwave radiation measurements (Rlw, Rpile, Tcase) at dcs come through the PI's data logger. Tcase for these measurements is resistance, not degrees Celsius. These data were not quality controlled and data availability is 100%.

All other radiometers were supplied by ISFS and provide measurements of the response of the thermopile within the radiometer dome (Rpile). Refer to **Table 7** for final data availability statistics after quality checks for the ISFS-controlled sensors. We derive an Rlw product from the Rpile and Tcase measurements to be consistent with the PI data logger measurements. These are included in the netcdf files.

Supersites - The Kipp&Zonen radiometers at 0.5 m had to be releveled a few times throughout the project. They were mounted separately on a boom fixed to a steel post (**Photo 1**). Unfortunately, dates and times when releveling occurred were not recorded. Comparisons between the 0.5 m and 2 m (see **Figure 10**) show offsets intermittently throughout the period of the project and at variable amplitudes. It is difficult to determine periods where the radiometers were not level. These data were not corrected.

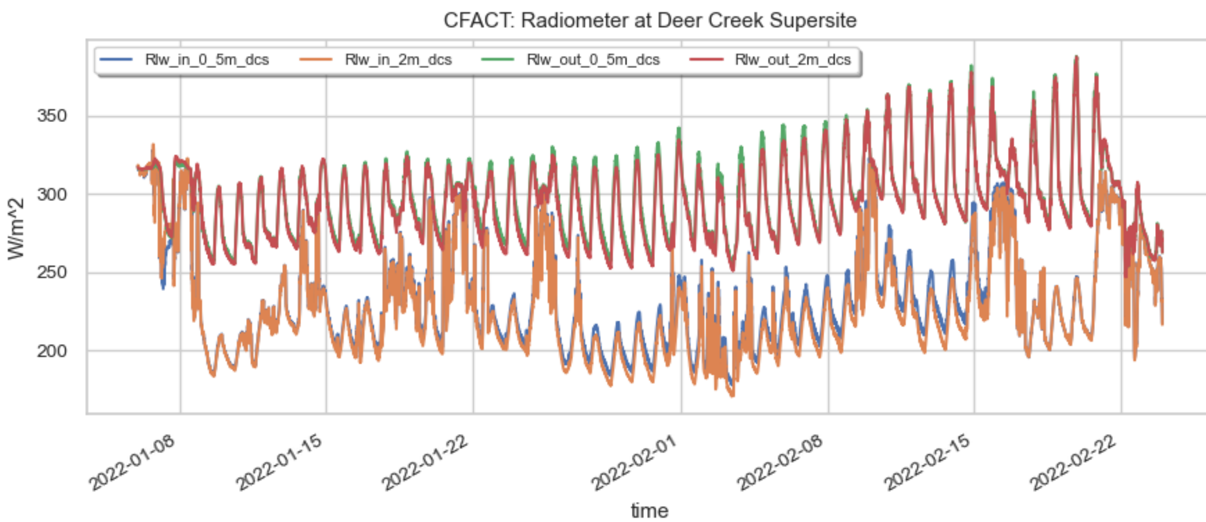

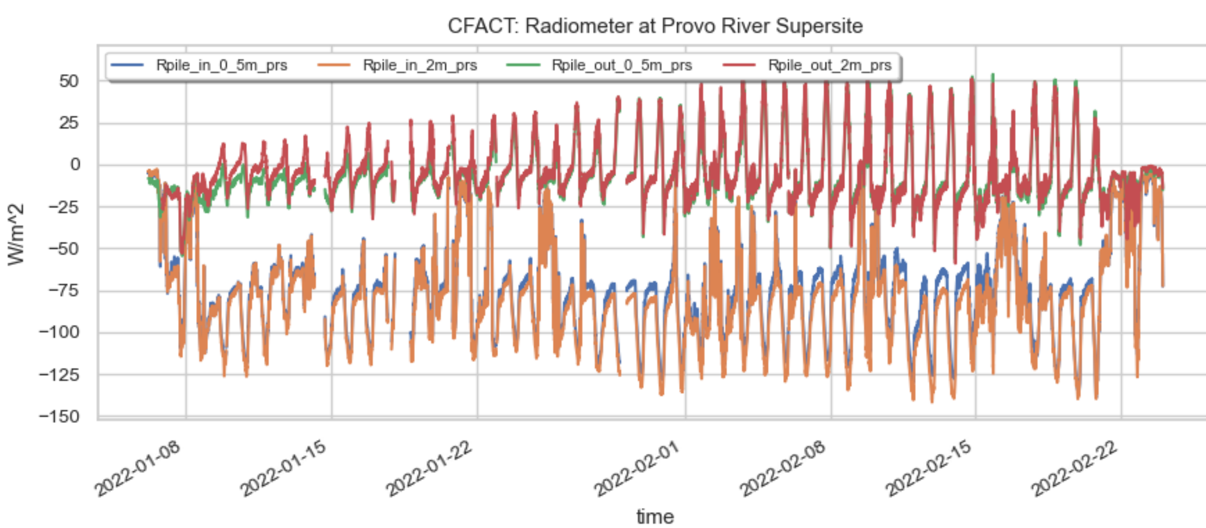

Figure 10. (top) incoming/outgoing longwave radiation at the Deer Creek Supersite. (bottom) incoming/outgoing thermopile variables (Rpile) at the Provo River Supersite.

Radiometer Calibrations

Due to scheduling and other constraints, the Kipp&Zonen radiometers were deployed preloaded with calibrations from at least 8 years prior, but were set up against NOAA standards at NOAA's Table Mountain Observatory, north of Boulder, during the summer following CFACT.

For short-wave radiation, we compared NOAA's reference values (the weighted sum of direct plus diffuse radiation) with our Kipp&Zonen readings when the zenith angle was within 1 degree of 45 degrees. The average ratio of these values is given in the **Table 10** below. The Kipp&Zonen readings have been divided by these ratios in the final data set.

Table 10. Kipp&Zonen comparisons with the NOAA standard radiometer.

Sensor ID	CFACT location	Gain, with respect to NOAA direct+diffuse
55	in.2m.prs	1.016
56	out.2m.dcs	1.019
57	spare	1.012
59	in.2m.dcs	1.013
5a	out.2m.prs	1.016
5b	spare	1.016

For long-wave radiation, we compared NOAA's long wave reference to our Kipp&Zonen readings by computing a reference Rpile.ref = Rlw.NOAA - sigma T_case.kz^4 (where T_case.kz is the case temperature from each of our Kipp&Zonen pyrgeometers) and then calculating the average ratio of Rpile from each Kipp&Zonen to Rpile.ref. To avoid needing to determine a short-wave correction to NOAA's values, we only used night-time data. Again, these ratios are shown below in **Table 11** and have been applied to our Kipp&Zonen Rpile values in the final data set. Note that for ID 6a, used as out.2m.prs, the Rpile signal during the Table Mountain calibration did not read correctly (although it appeared to work fine during all of CFACT). For this sensor, we left the Rpile gain at 1.000.

Table 11. Corrections applied to Kipp&Zonen Rpile variable.

Sensor ID	CFACT usage	Rpile gain
64	in.2m.prs	0.967
65	out.32m.prs	0.960
66	in.0.5m.prs	0.987
67	out.7m.prs	1.020
68	in.7m.prs	0.977
69	in.32m.prs	0.990
6a	out.2m.prs	-
6b	out.0.5m.prs	1.033

Radiometer Intercomparison

During the period 23 Dec - 5 Jan, the Kipp & Zonen and NR01 radiometers were operated all at a height of 2m at each of the 2 supersites (dcs and prs). Incoming radiometers were left as incoming and outgoing as outgoing. For shortwave radiation, this was no change and was simply a comparison of the Kipp & Zonen vs. the NR01 at each site. There are large differences between these shortwave values during the day (>30 W/m^2), which likely indicated that the NR01 was tilted, at least at prs. As of this writing, the dcs Rsw values during the intercomparison are not available.

For longwave radiation, differences between the Kipp&Zonens at prs were mostly within 1 W/m^2, after the adjusted gains above were applied. The NR01 differences were 5 W/m^2 or more, again suggesting that the NR01 was tilted. At dcs, differences between the Kipp&Zonens were up to 5 W/m^2 and typically 10 W/m^2 for the NR01. However, the dcs Kipp & Zonen gains have not been changed since these sensors were not NCAR's and were not part of the Table Mountain calibration.

3-D Sonic anemometer - CSAT3

CSAT3 sonic anemometers were used for turbulence measurements on all towers. The orientation of each sonic was calculated using the Leica theodolite and a handheld compass. **Figure 11** is a time series of the wind speed. The wind speed component is representative of the data availability of the sonic measurement system.

08 January 2022 - Bad sonic at Soldier Hollow (sh) was replaced.

11 January 2022 - Provo River Supersite (prs) sonic at 2 m was rewired to another data systems module to get it operating.

Lake Creek (lc) - significant data gaps observed at lc for the sonic and h2o/co2 infrared gas analyzer due to bad sensors.

- 09 February - replaced the EC100 which did not solve occurrences of data gaps.
- 19 February - replaced the CSAT3A sonic with the PI-supplied sensor, however we had to adapt how we bolted this sonic to the boom because the clamps were different from ours.

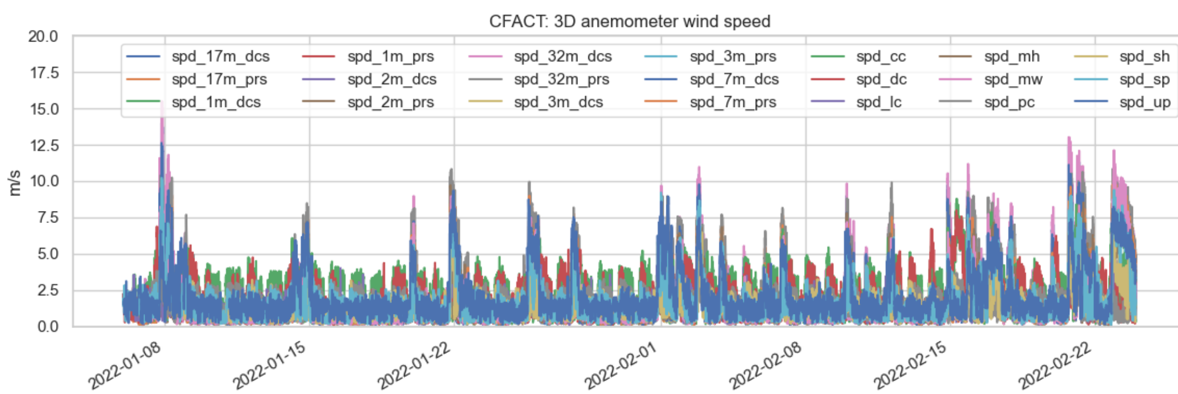

Figure 11. Final 5-minute CSAT3 wind speed time series for the period of field operations.

Sonic Calibrations

Sonic anemometers were calibrated using the EOL Wind Tunnel. Anemometers were calibrated over temperatures from -30°C to +50°C at RH=0%. The anemometers were calibrated with three orientations (on the x, y, z axes) and the u component was examined. Overall, the u component measured deviations between 0.0 cm/s and 0.3 cm/s with a standard deviation of +/- 0.1 cm/s. Calibrations were conducted in July and August 2022.

H_2O/CO_2 infrared Gas Analyser (IRGA)

CSAT3 was coupled with an infrared absorption gas analyzer (EC-150 IRGA) to measure H_2O and CO_2.

The sensors were filtered for
- irgadiag not equal to 0
- Negative spikes, particularly for H_2O.

We observed a significant number of negative spikes in H_2O density (g/m^3) data stream which contributed to a ~ 2% additional reduction of data in each variable's time series. The exception was at the Deer Creek supersite which recorded an 11% drop in data recovery in H_2O at 7 m. There were no negative spikes in the CO_2 density measurements. We observed very few positive spikes overall. **Figure 12** time series of final data after diagnostics (irgadiag variable and min/max value limits) were applied to H_2O and CO_2. We observe a high bias in h2o at 17m at the prs site (h2o_17m_prs, orange in **Figure 12b**). This bias is about 3-4 times higher than average. We have not applied a bias correction.

No other significant problems were noted during operations. No sensors were replaced during operations.

(A)

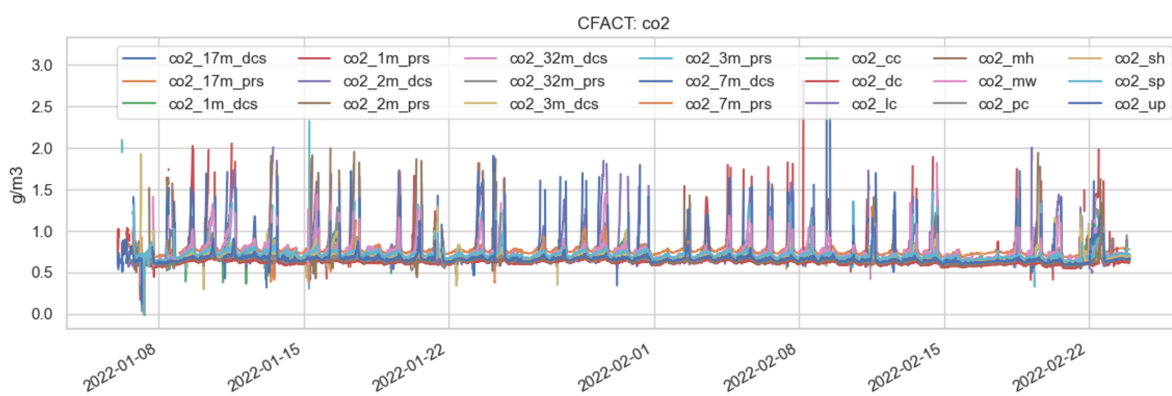

(B)

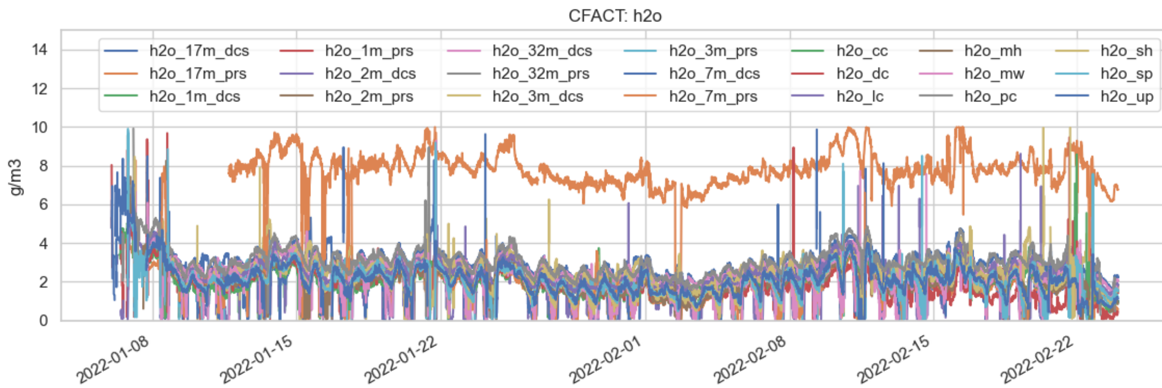

Figure 12. Time series of EC-150 IRGA (A) co2 and (B) h2o.

Soils

All soil sensors (NCAR 4-level Tsoil, Meter EC-5 Qsoil, REBS HFT Gsoil, and Hukseflux TP01 thermal properties) were buried at 0 – 5 cm layer near the base of towered sites. Refer to documentation on the installation of soil sensors for more details.

We theorize that observed late afternoon spikes in dc, lc, sp, and mw sites are real following rapid daytime heating at sunrise followed by rapid cooling at sunset.

Heat flux, Gsoil

No problems noted during operations. No problems were found during QC processing. No sensors were replaced during operations.

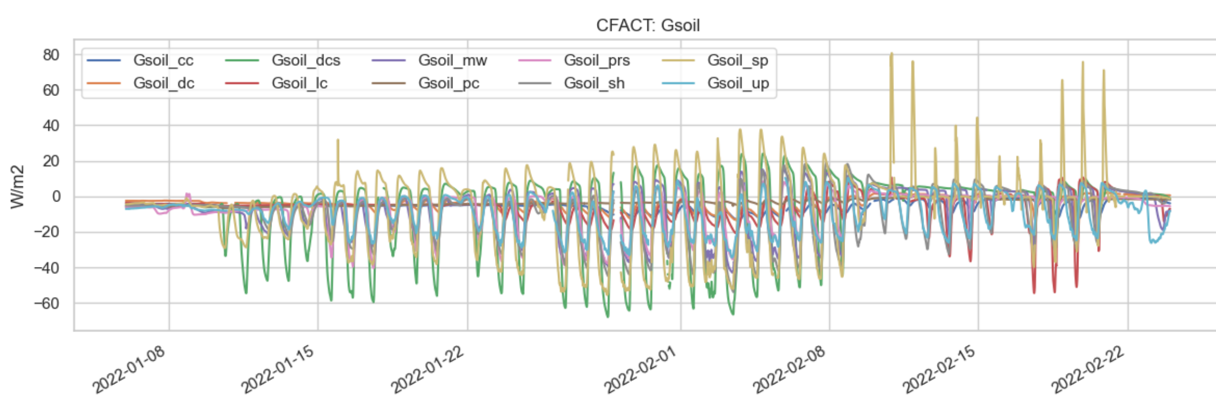

Figure 13. Time series of Gsoil at each site.

Soil Temperature, Tsoil

Tsoil sensors were installed at depths of 0.6 cm, 1.9 cm, 3.1 cm and 4.4 cm. Data at Soldier Hollow (sh) were corrected for communication glitches between the Tsoil and the mote by filtering bad messages in the raw data. No other problems noted during operations. No sensors were replaced during operations.

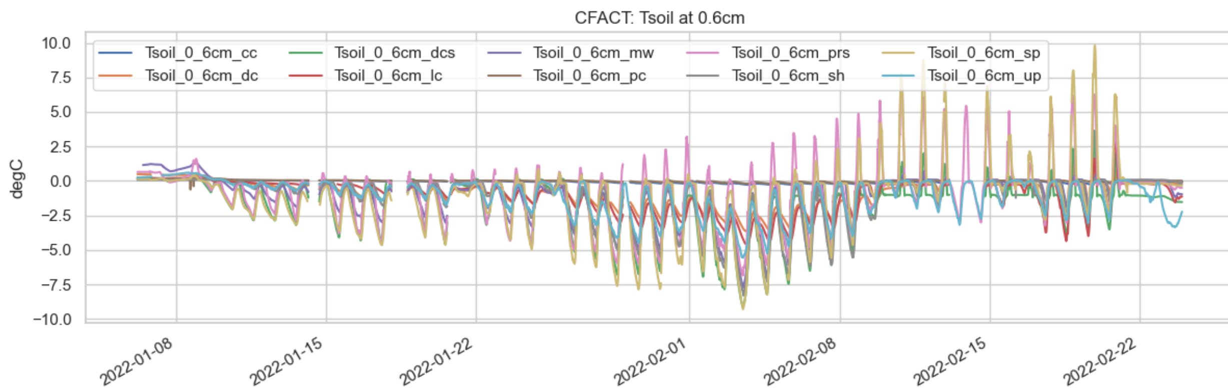

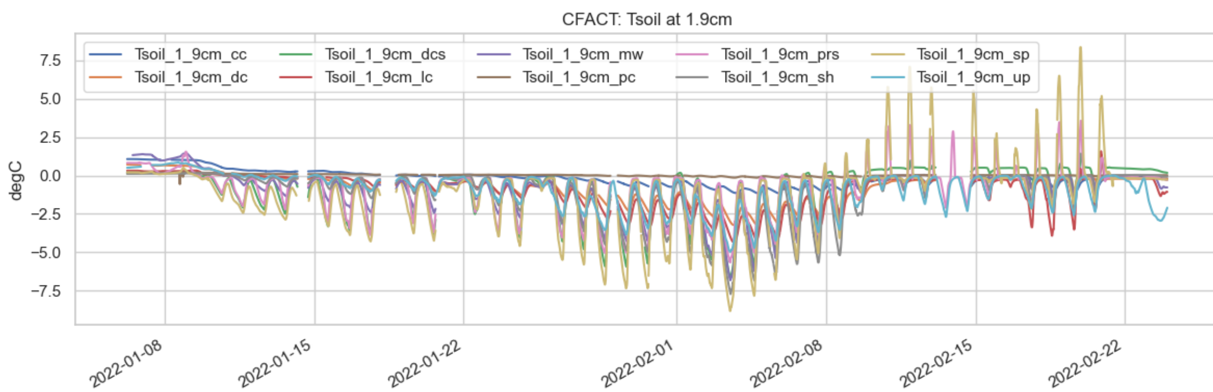

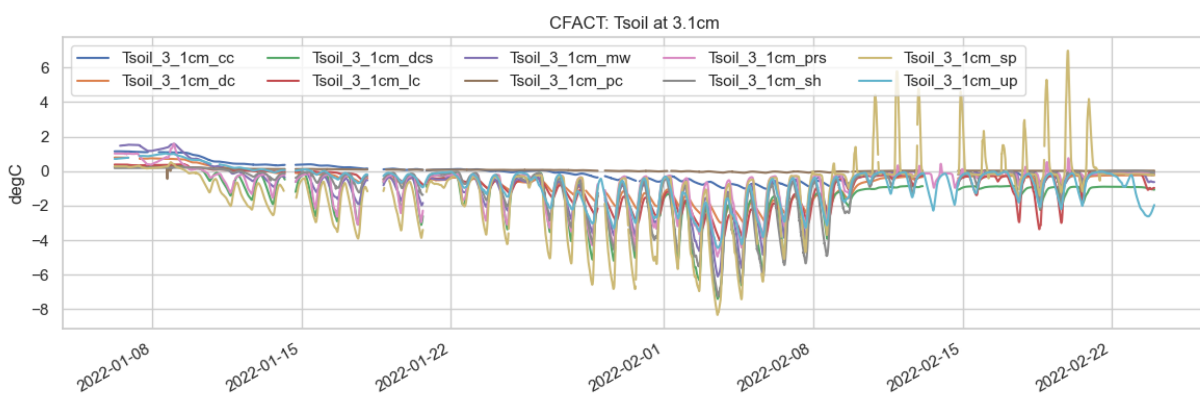

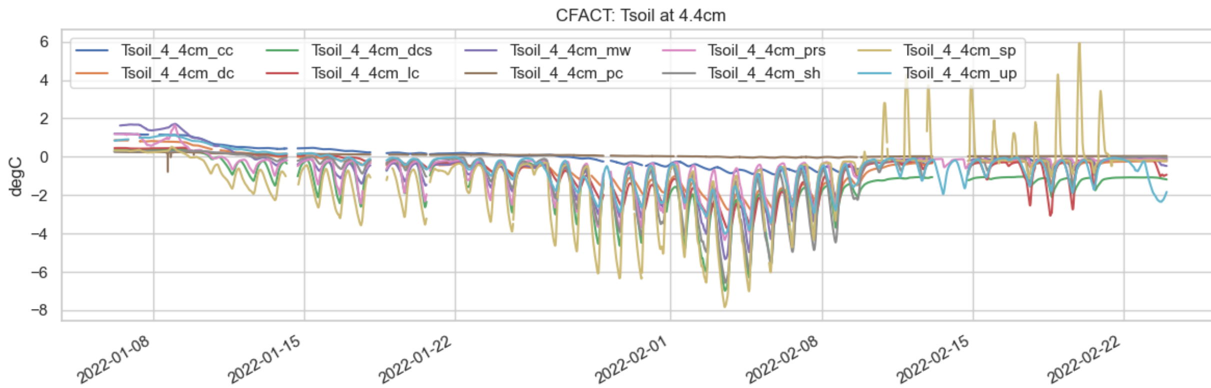

Figure 14. Time series of Tsoil at each height level.

Soil Moisture, Qsoil

The soil moisture sensor (Qsoil) was installed at a depth of 2.5 cm. We used the manufacturer's calibration values for potting soil.

Freezing conditions made it difficult to gather a 3rd soil sample. After freezing occurs, soil moisture values cannot be trusted. Tsoil at 3.1 cm and Qsoil for each site was plotted and the transition date was recorded where Tsoil temperatures first dip below freezing. Qsoil data was removed after that transition date. **Table 12** shows cut-off Qsoil dates. **Figure 15** shows the resulting time series of Qsoil at each site.

Qsoil data at dcs was removed due to bad measurements since installation. It was not possible to replace the sensor since the ground was quite hard prior to the start of the project and we were concerned about disturbing nearby soil sensors.

Table 12. Cut-off dates for Qsoil at each site where Tsoil temperatures first dip below freezing.

Site	Date
cc	Jan 23
dc	Jan 13
dcs	Jan 10
lc	Jan 13
mw	Jan 11
pc	Jan 29
prs	Jan 10

sh	Jan 11
sp	Jan 9
up	Jan 13

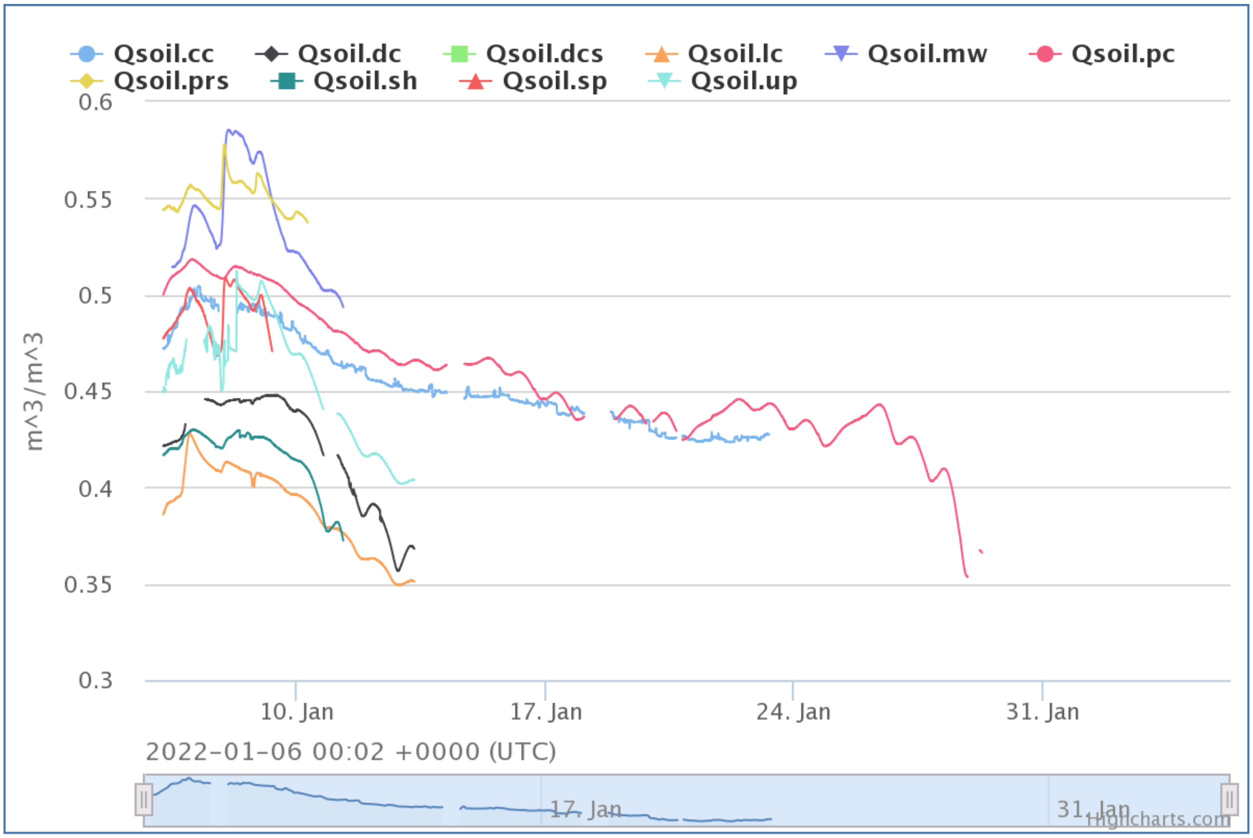

Figure 15. Time series of final Qsoil at each site.

Thermal conductivity (Lambda) and Decay time constant (Tau63)

No problems noted during operations. No problems were found during QC processing. No sensors were replaced during operations.

Rain rate, OTT

All sensors performed well. No problems noted during operations. No problems were found during QC processing. No sensors were replaced during operations. Sensors internal processing and flagging accounts for the lower data availability.

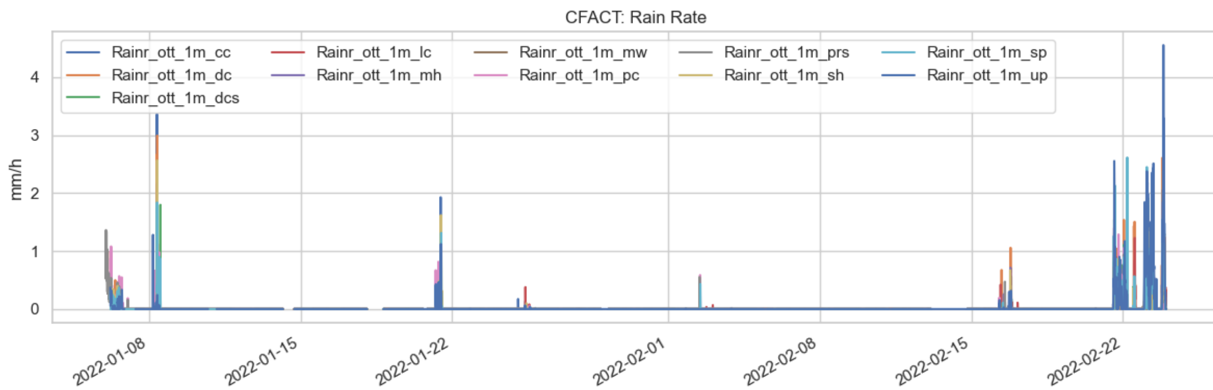

Figure 16. Time series of rain rate at each site.

PI-supplied Sensor Data

HRXL Snow Depth

The HRXL snow depth gauges instruments are PI owned. The minimum snow depth is used in this dataset as the best choice for snow surface heights. An offset height of each snow depth sensor was measured from the tower base plate to the HRXL sensor midpoint to establish initial conditions (See **Photo 3**). These heights are estimates taken with a measuring tape and reflect lengths taken during field operations, i.e. not taken immediately after set-up (**Table 13**). Thus, these values may not accurately reflect the actual snow depths. It is recommended to use these data for qualitative analysis only. These data have been filtered for negative heights that may reflect the inaccuracy of our offset measurements.

Snow depth measurements were removed from the Memorial Hill (mh) site due to interference with surrounding shrubs and the tool storage chest (job box). Refer to **Photo 4** of the mh site.

Snow depth at the Upper Provo (up) was noisy relative to the other sites, thus we recommend using these data with caution. Note there may be interference with low lying grass affecting the measurements. It is recommended to use these data for qualitative analysis.

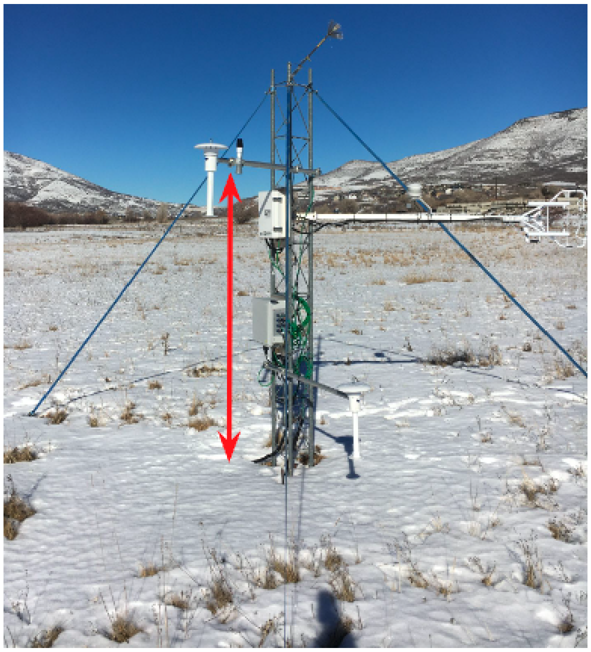

Photo 3. Illustration of a typical height measurement of the HRXL taken at Upper Provo.

Photo 4. View of the Memorial Hill site, looking W.

Table 13. Heights of the HRXL snow depth sensor taken from the tower base plate to the midpoint of the sensor.

Site	Height [cm]
cc	233
dc	230
dcs	205
lc	232
mh*	231
mw	231
pc	233
prs	207
sh	232
sp	234
up	232

*Though measured, data were removed due to interference.

Campbell C125 Visibility

The C125 visibility sensor was designed to detect fog. These data have been left as is.

There will be differences between visibility measurements estimated by the Ott and that from the CS125. The Ott is designed to measure precipitation and only measures droplets down to about 0.2 mm, much larger than typical cloud/fog droplets (around the 10 - 20 microns range, ie, ten times smaller). The Ott visibility is more a measure of the visibility due to precipitation, whereas the CS125 is designed to detect fog. Since snowfall was minimal during CFACT it is recommended to use the CS125 visibility measurements for fog detection.

Thermocouples

PI-supplied thermocouples (Campbell Scientific FW1) were mounted on satellite and supersites towers. Data are noisy at 1 m and 3 m at Deer Creek and at 1 m, 2 m, 3 m at Provo River prior to replacing them on 10 January 10 2022 and should be ignored. A few spikes at the beginning of the project have been removed from several sites' time series.

Thermocouple used at CFACT were wire style sensors that were prone to breaking. There was a limited supply of sensors that it was decided to focus on replacing broken thermocouples only at the supersites. Refer to **Table 8** for dates and times of the lower/raising of the towers to replace inoperable thermocouples.

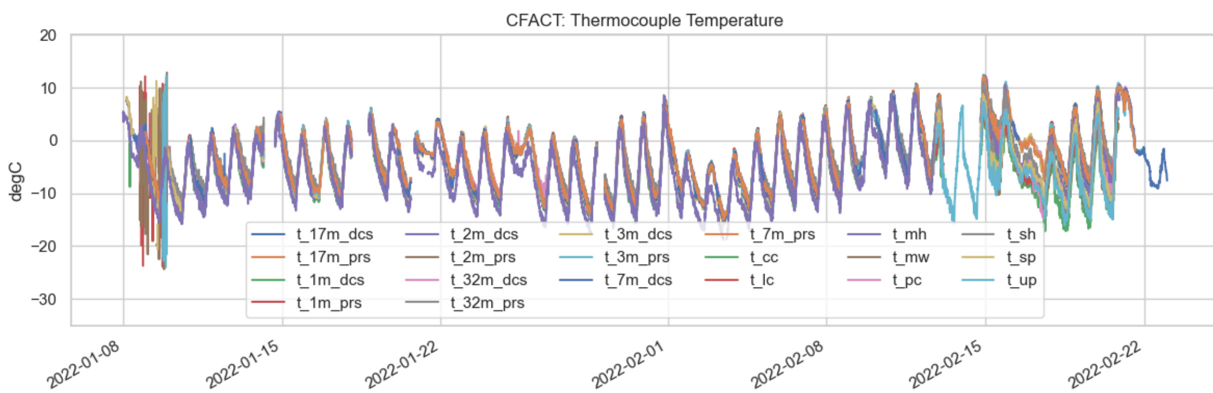

Figure 17. Time series of thermocouple temperature at each site.

Intensive Operating Periods (IOPS)

The study period of the project experienced only light fog events with the exception of IOP9 during the last days of the project. The event is evident in the rain rate time series in **Figure 16**.

IOP1 - Ephemeral fog - Tues/Wed Jan 11-12 2022

IOP2 - Clear - Sun/Mon Jan 16-17 2022

IOP3 - Ephemeral fog - Wed/Thurs Jan 19-20 2022

IOP4 - Ice fog - Thurs/Fri Feb 3-4 2022

IOP5 - Moisture surge - Wed/Thurs Feb 9-10 2022

IOP6 - Ephemeral fog - Sat/Sun Feb 12-13 2022

IOP7 - Ephemeral fog- Thurs/Fri Feb 17-18 2022

IOP8 - Ephemeral Fog - Fri/Sat Feb 18-19 2022

IOP9 - Ephemeral - Wed/Thurs Feb 23-24 2022

Bonus - Ephemeral - Sat/Sun Feb 26-27 2022